PHYSICAL REVIEW A VOLUME 34, NUMBER 5 NOVEMBER 1986

Stark broadening of H_α and H_β lines of C^{5+}

Dipak H. Oza
Center for Radiation Research, National Bureau of Standards, Gaithersburg, Maryland 20899

Ronald L. Greene
Department of Physics, University of New Orleans, New Orleans, Louisiana 70148

Daniel E. Kelleher*
Joint Institute for Laboratory Astrophysics, National Bureau of Standards and University of Colorado, Boulder, Colorado 80309-0440

(Received 11 June 1986)

We have computed the Stark-broadened profiles of the first two Balmer lines ($n=3,4\rightarrow 2$) of C^{5+}. Plasma conditions span the electron density range $n_e=10^{17}$–10^{20} cm^{-3}, and $T=20$–300 eV. The calculations include ion-dynamic effects, which we find are very important at the lower densities for H_α ($n=3\rightarrow 2$). At the higher densities, the dynamic profiles approach the static ones.

I. INTRODUCTION

In the mid seventies experimental observations revealed that the motion of the perturbing ions with respect to hydrogenic radiators had a significant effect near the center of the profile.[1] This effect was observed to increase the width of the H_α line and fill in the "dip" in the H_β line. Up to that time, computations had assumed the ions to be quasistatic.

This was followed by a period of intensive theoretical work on the so-called "ion-dynamic" problem. The main difficulty is that strong ion collisions overlap in time for the range of plasma conditions that were being considered. This problem requires that the theoretical approach must incorporate time-dependent many-body ion interactions for an accurate and realistic description of the processes involved. The treatment of static ion fields has been well in hand for some time, as has the "impact" broadening by the fast moving electrons, whose collisions are generally binary. However, the problem of time-dependent many-body ion interactions has eluded analytical treatment to the present.

Recently, it was observed that for some plasmas containing high-Z hydrogenic radiators, it is possible for dynamic ion perturbations to be extremely important, leading to collisional linewidths orders of magnitude larger than those predicted using static ions.[2] In particular, when the high-Z radiators are perturbed by low-Z ions, line profiles having significant unshifted components can be strongly affected. The fields $\mathcal{E}(t)$ from the time-dependent many-body interactions can be accurately approximated by molecular dynamics simulations. In Ref. 2, once the $\mathcal{E}(t)$ were estimated, the authors performed a numerical solution to the coupled equations for the time-development operator. From this the line shape was obtained via Fourier transformation. This numerical approach takes on an enormously larger scale when the lower level of the transition is other than the ground state, and to date only Lyman lines have been computed using these numerical methods.

Balmer lines are important in many applications, including recombination x-ray lasers, electron density diagnostics, and radiative transfer. For example, Suckewer *et al.*[3] have demonstrated an enhancement of ~ 100 in stimulated emission over spontaneous emission of the CVI 182-Å line (H_α) in a recombining, magnetically confined plasma. In the recombining phase, the electron temperature is about 20 eV and the electron density about 5×10^{18} cm^{-3}. In this Rapid Communication, we address the question of ion-dynamic effects for Balmer-α and -β lines ($n=3$, $4\rightarrow 2$) of C^{5+} for electron densities ranging from 10^{17} to 10^{20} cm^{-3} for the temperatures of 20 to 300 eV.

To compute Balmer lines with ion dynamics, we have applied the semianalytical method of Greene.[4] The ion field $\mathcal{E}(t)$ is still estimated by numerical simulation, but we utilize an analytical solution for the time-development operator, using fitting functions for moments of the electric field. In addition to ion-dynamic effects, the calculation includes lower state interference and broadening. An adiabatic-type approximation is made, but at a point in the formalism where large errors are not expected. A more detailed summary of the theory is given below.

II. THEORY

As noted in Ref. 4, the principal quantity of interest in the calculation of the line shape is the Fourier transform of the ensemble average of the time-development operator:

$$\langle U(\omega)\rangle \equiv \int_0^\infty dt\, e^{i\Delta\omega t}\langle U(t,0)\rangle \ . \tag{1}$$

Here $\langle\ \rangle$ represents an average over ion perturbers only. Tetradic operators are used in this expression, so that the effects of broadening of the lower state can be included for lines beyond the Lyman series.[5] The quantity $\Delta\omega$ is the frequency separation from line center. We treat the electrons with the impact approximation. After the averages over electron perturbers, the time-development operator

$U(t,t')$ satisfies[6]

$$i\frac{\partial U(t,t')}{\partial t}=[V(t)+i\phi]U(t,t') \ . \tag{2}$$

For convenience, we take $\hbar=1$ in this section. Correlation between electron and ion perturbers is approximated through the use of Debye screening, in that each perturber is treated as an independent, screened quasiparticle. In Eq. (2), $V(t)$ is the total (shielded)ion-radiator interaction, and ϕ is the electron impact operator. For the present calculations we use the time-ordered expression for ϕ given by Greene.[7]

The effects of ion broadening can be treated with a relaxation theory described in Refs. 4 and 8. In this formalism the ion-broadening operator $M_I(\omega)$ is defined by the equation

$$\langle U(\omega)\rangle\equiv[\Delta\omega-i\phi-iM_I(\omega)]^{-1} \ . \tag{3}$$

This operator is given in terms of $V(t)$ and $U(t,t')$ by the following expression:[4]

$$M_I(\omega)=-\int_0^\infty dt\, e^{i\Delta\omega t}\langle V(t)U(t,0)V(0)\rangle \times\left[1-i\int_0^\infty dt\, e^{i\Delta\omega t}\langle U(t,0)V(0)\rangle\right]^{-1} \ . \tag{4}$$

If the dipole approximation is made to the ion-radiator interaction $V(t)$, the perturber averages in Eq. (4) can, after an adiabatic-type assumption, be approximated by[4,8]

$$\langle V(t)U(t,0)V(0)\rangle\simeq\int_0^\infty dE\int\frac{d\Omega_0}{4\pi}D^{-1}(\Omega_0)d_z\exp(id_zEt+\phi t)d_zD(\Omega_0)F(E,t) \tag{5a}$$

and

$$\langle U(t,0)V(0)\rangle\simeq-\int_0^\infty dE\int\frac{d\Omega_0}{4\pi}D^{-1}(\Omega_0)\exp(id_zEt+\phi t)d_zD(\Omega_0)G(E,t) \ . \tag{5b}$$

$D(\Omega_0)$ is a rotation operator with Ω_0 representing the angles θ_0,ϕ_0 of the rotation. The quantity d_z is the z component of the atomic dipole moment operator.

The field-dependent quantities $F(E,t)$ and $G(E,t)$ are given by

$$F(E,t)=\left\langle\mathcal{E}(t/2)\cdot\mathcal{E}(-t/2)\delta\left[E-\frac{1}{t}\int_{-t/2}^{t/2}dt'\mathcal{E}(t')\right]\right\rangle \ , \tag{6a}$$

$$G(E,t)=\left\langle\frac{\mathcal{E}(t/2)\cdot\mathcal{E}(-t/2)}{\mathcal{E}(t/2)}\delta\left[E-\frac{1}{t}\int_{-t/2}^{t/2}dt'\mathcal{E}(t')\right]\right\rangle \ , \tag{6b}$$

where $\mathcal{E}$ represents the total (screened) electric field due to the ions and $\mathcal{E}=|\mathcal{E}|$.

We evaluate $F(E,t)$ and $G(E,t)$ using a Monte Carlo procedure similar to that of Stamm and Smith.[9] In this procedure we randomly place ions inside a sphere of radius $5r_0$, where r_0 is the mean ion spacing defined by $4\pi n_i r_0^3/3=1$.

In this procedure each of the randomly placed ions is given a velocity selected randomly via the Maxwellian velocity distribution, and moved along a straight-line path determined by that velocity. [The straight-line path approximation has been examined by Greene[8] and shown to be valid in the nonbinary regime, as long as $Z_rZ_p^{2/3}a^2/9\ll1$, where Z_r and Z_p are the radiator and ion perturber charges, and $a=r_{0e}/\rho_D$ is the screening parameter $(4\pi r_{0e}^3n_e/3=1)$.[9,10] For our case we have $Z_r=5$, $Z_p=5$, and $a\cong0.2$ (depending on plasma conditions), so that the condition is satisfied.] The field quantities $\mathcal{E}(t/2)\cdot\mathcal{E}(-t/2)$ and $\mathcal{E}(t/2)\cdot\mathcal{E}(-t/2)/\mathcal{E}(t/2)$ are evaluated at the center of the sphere and sorted according to the value of the integral

$$\frac{1}{t}\int_{-t/2}^{t/2}dt'\mathcal{E}(t') \ ,$$

estimated with the trapezoidal rule. For these conditions we have used 50000 initial configurations.

After $F(E,t)$ and $G(E,t)$ are calculated for various values of t, they are fitted to functions proportional to

$$f(E,t)=[1+a(E)t+b(E)t^2+c(E)t^3]e^{-\gamma(E)t} \ , \tag{7}$$

where $a(E)$, $b(E)$, $c(E)$, and $\gamma(E)$ are adjustable parameters. The functions which are fitted to the calculated values of $F(E,t)$ and $G(E,t)$ are constrained to give the correct $t=0$ values. These $t=0$ values correspond to the static ion microfield distributions $P(\mathcal{E})$ for a charged point of $Z_r=5$ and are computed using the code of Tighe and Hooper.[10] The details of this procedure, including its benefits and estimated errors, are discussed in Ref. 4.

III. RESULTS AND DISCUSSION

Results for the H_α $(3\rightarrow2)$ transition in C^{5+} are shown in Fig. 1, in which computations treating the ions as static are included for comparison. We assume that all ion perturbers are C^{5+}. It is clear that ion-dynamic effects dominate the width at lower electron densities. At $n_e\gtrsim10^{21}$ cm^{-3}, the "dynamic" and static widths become essentially equal for a temperature of 20 eV. The "ion-impact" limit[11] is also included in Fig. 1 at $n_e=10^{17}$ cm^{-3}, using the Debye length[2]

$$\rho_D=[kT/4\pi e^2n_e(1+Z_p/2)]^{1/2} \ . \tag{8}$$

This density is still somewhat beyond where the impact validity is satisfied, so the excellent agreement between the dynamic and impact result is expected to be fortuitous to a certain extent.

For the lines observed at the lower densities in the graph (Fig. 1), the broadening caused by any collisional effects is dwarfed by the thermal Doppler width. (Griem has recently treated possible deviations from thermal Doppler

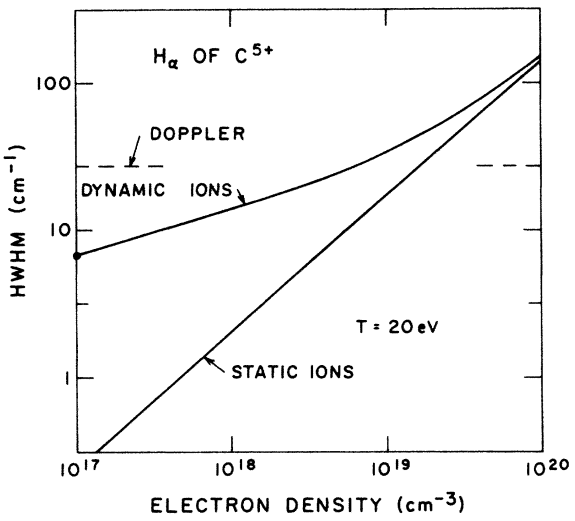

FIG. 1. Half the width at half maximum (HWHM) of the H_α line of C^{5+} at $T=20$ eV. The line labeled "dynamic ions" represents the results of the complete calculation. Results from the "static-ion" and "ion-impact" limits (●) are included for comparison.

broadening.[12]) However, in the density range from about 5×10^{18} cm^{-3} to a little more than 10^{19} cm^{-3}, the relative importance of Doppler and Stark broadening is qualitatively different in the two different physical schemes of approximations, viz., quasistatic ions and dynamic ions. It is in this density range that the inclusion of ion-dynamic effects becomes crucial for a realistic theoretical estimate of the line-broadening phenomenon.

The temperature dependence of the half width including ion dynamics is indicated in Fig. 2. At the higher temperature of 300 eV, the ion-dynamic effects are quite significant at $n_e \simeq 10^{20}$ cm^{-3}, unlike at $T=20$ eV. The ratios of ion-dynamic half width to the quasistatic half width is about 4.0 at $T=300$ eV as opposed to 1.1 at $T=20$ eV.

The Balmer-α transition consists of seven fine-structure components. Most of the oscillator strength occurs in the $3d_{5/2}$-$2p_{3/2}$ and $3d_{3/2}$-$2p_{1/2}$ transitions, which are separated by 428 cm^{-1}.[13] This is larger than the collisional broadening of the H $_\alpha$ line at the densities indicated in the figure, so the spectrum will appear approximately as overlapping Lorentzians. However, we expect that the broadening indicated in the figure (where fine structure has been ignored) represents reasonable estimations of the width of each of these components, at least for the higher densities. This is because the important splittings for the line broadening are between the $3p$ and $3d$ sublevels; the $3p_{3/2}$-$3d_{3/2,5/2}$ splittings are 0.2 and 47 cm^{-1}, respectively.[13] For the higher densities, at least, even the larger splitting is small enough to make the sublevels quasidegenerate. Computations including fine structure are planned.

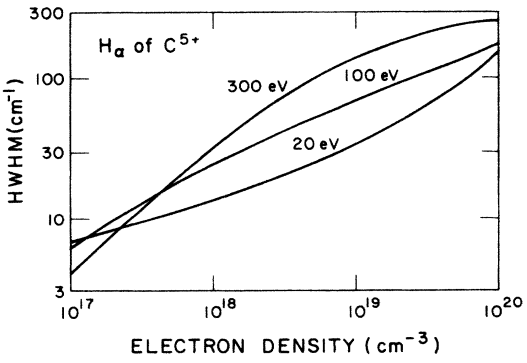

FIG. 2. HWHM of the H_α line of C^{5+} at $T=20$, 100, and 300 eV as a function of electron density. Ion-dynamic effects are included.

We have also performed calculations of the collisional broadening of the H_β ($n=4\rightarrow 2$) line of C^{5+}. While the H_α line is of primary interest as, for example, a lasing transition, the H_β line is generally more useful as a plasma diagnostic tool of the charged particle density. This is because it is broader than the H_α line, and therefore much less influenced by Doppler broadening and self-absorption. The H_β line has a dip in line center, because unlike H_α it has no unshifted Stark components. Therefore, the two peaks of the H_β profile are on either side of the line center, with the result that the half width and peak separation are rather insensitive to ion dynamic effects. The half width at half maximum and (full) peak separation are displayed in Fig. 3. The fine structure of the lower ($n=2$) level should still be accounted for when comparing these results to experimental data.

We estimate the uncertainty in the width of the H_α line to be possibly a factor of 2 (somewhat less at the higher densities and somewhat more at the lower densities). The main sources of this uncertainty, in order of importance, are fine structure effects, approximations in the formalism, and the assumption of straight-line perturber paths. In comparing them with experimental results, one should recall that our calculations assume that all the ion per-

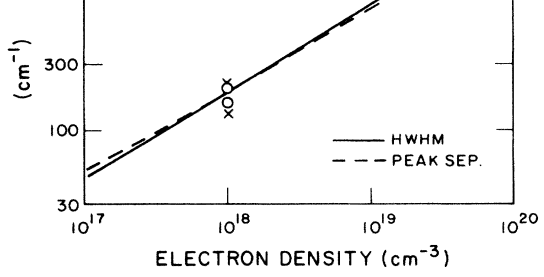

FIG. 3. Half the width at half maximum (HWHM) (solid line) of the H_β line of C^{5+} at $T=100$ eV as a function of electron density. The open circles (○) below and above the line indicate the HWHM at 20 and 300 eV, respectively, at $n_e=10^{18}$ cm^{-3}. Also shown is the full separation of the two peaks (dashed line) of the H_β line at $T=100$ eV as a function of electron density; the crosses (×) below and above the line indicate the peak separation at 20 and 300 eV, respectively. This peak separation can serve as a plasma diagnostic which is complementary to the HWHM but less sensitive to optical depth and linearity of the photodetection.

turbers are C^{5+}. Also, contributions from any possible plasma turbulence have not been considered in our calculation. It should be possible to reduce the uncertainty significantly through improvements in each of the above sources of error. Future efforts in this direction are being planned. In the meantime, we believe that our present results should prove useful for many applications.

In closing we wish to point out an interesting qualitative feature of the reduced mass dependence of the ion-dynamic effect for hydrogenic radiators. In the quasistatic-ion regime there is of course no dependence on the reduced mass μ of the radiator and ion perturber. There are two different dynamical regimes, however, which display very different dependence on the reduced mass. The regime most accessible to experimental observation so far has been for electron densities somewhat below that where the ions behave quasistatically. In this region, the ion-dynamic effect has been observed to scale roughly as $\mu^{-1/2}$,[1] consistent with the fact that the lighter the ion, the faster it moves, and the larger the dynamical effect. If, however, the density is sufficiently low that the ions are in the impact regime, the impact width scales as $\mu^{1/2}$,[11] reflecting the fact that the impacts of slower ions last longer, giving rise to a larger Stark effect. In the intermediate region (collisional rate $\approx$ ion plasma frequency), one thus expects a relatively weak dependence on μ, even though the ion-dynamical effect is typically quite large in this regime.

ACKNOWLEDGMENTS

We gratefully acknowledge many useful discussions with J. Cooper. We also thank L. A. Woltz for providing the computer code to generate the static microfield distributions (Ref. 10). This work is supported in part by the U.S. Air Force Office of Scientific Research Contract No. ISSA86-0014. One of us (D.E.K.) acknowledges the support of the JILA/NBS Exchange Fellow Program.

*Permanent address: Center for Radiation Research, National Bureau of Standards, Gaithersburg, MD 20899.

[1]D. E. Kelleher and W. L. Wiese, Phys. Rev. Lett. **31**, 1431 (1973); W. L. Wiese, D. E. Kelleher, and V. Helbig, Phys. Rev. **11**, 1854 (1975).

[2]R. Stamm, Y. Botzanowski, V. P. Kaftandjian, B. Talin, and E. Smith, Phys. Rev. Lett. **52**, 2217 (1984); R. Stamm, B. Talin, E. L. Pollock, and C. A. Iglesias, this issue, Phys. Rev. A **34**, 4144 (1986). This effect for high-Z radiatiors was previously predicted, R. L. Greene, J. Phys. B **15**, 1831 (1982).

[3]S. Suckewer, C. H. Skinner, H. Milchberg, C. Keane, and D. Voorhees, Phys. Rev. Lett. **55**, 1753 (1985).

[4]R. L. Greene, J. Quant. Spectrosc. Radiat. Transfer **27**, 639 (1982).

[5]C. R. Vidal, J. Cooper, and E. W. Smith, J. Quant. Spectrosc. Radiat. Transfer **10**, 1011 (1970).

[6]D. Voslamber, Phys. Lett. **61A**, 27 (1977).

[7]R. L. Greene, Phys. Rev. A **14**, 1447 (1976).

[8]See Ref. 2, Greene.

[9]R. Stamm and E. W. Smith, Phys. Rev. A **30**, 450 (1984).

[10]C. F. Hooper, Phys. Rev. **165**, 215 (1968); R. J. Tighe and C. F. Hooper, Phys. Rev. A **15**, 1773 (1977).

[11]C. Sthele, A. Mazure, G. Nollez, and N. Fourtrier, Astron. Astrophys. **127**, 263 (1983); C. Sthele, J. Phys. B **18**, L43 (1985).

[12]H. R. Griem, Phys. Rev. A **33**, 3580 (1986).

[13]S. Bashkin and J. A. Stoner, *Atomic Energy Levels and Grotrian Diagrams 1* (North-Holland, Amsterdam, 1975).